LETTERS
PUBLISHED ONLINE: 30 MAY 2010 | DOI: 10.1038/NPHYS1680
nature physics

Thermalization of a two-dimensional photonic gas in a 'white wall' photon box

Jan Klaers, Frank Vewinger and Martin Weitz*

Bose–Einstein condensation[1], the macroscopic accumulation of bosonic particles in the energetic ground state below a critical temperature, has been demonstrated in several physical systems[2–8]. The perhaps best known example of a bosonic gas, blackbody radiation[9], however exhibits no Bose–Einstein condensation at low temperatures[10]. Instead of collectively occupying the lowest energy mode, the photons disappear in the cavity walls when the temperature is lowered—corresponding to a vanishing chemical potential. Here we report on evidence for a thermalized two-dimensional photon gas with a freely adjustable chemical potential. Our experiment is based on a dye-filled optical microresonator, acting as a 'white wall' box for photons. Thermalization is achieved in a photon-number-conserving way by photon scattering off the dye molecules, and the cavity mirrors provide both an effective photon mass and a confining potential—key prerequisites for the Bose–Einstein condensation of photons. As a striking example of the unusual system properties, we demonstrate a yet unobserved light concentration effect into the centre of the confining potential, an effect with prospects for increasing the efficiency of diffuse solar light collection[11].

Following the achievement of atomic Bose–Einstein condensation[2–4], we have witnessed interest in light sources where a macroscopically populated photon mode is not the consequence of laser-like amplification, but rather results from a thermal equilibrium phase transition. Work in this direction includes the proposal of a superfluid phase transition of photons in a nonlinear cavity[12–14] and, albeit in the strong-coupling regime, the demonstration of a quasiequilibrium phase transition of exciton–polariton quasiparticles to 'half matter, half light' condensates[6–8]. In the weak-coupling regime (as in our case), optical cavities have been used to achieve a modified spontaneous emission of atoms and molecules[15–17].

The main idea of our experiment is to study thermalization of a photon gas, to a heat bath near room temperature (dye molecules), in a system with reduced spatial dimensionality and an energy spectrum restricted to values far above the thermal energy. The photons are trapped in a curved-mirror optical microcavity, and repeatedly scatter off dye molecules. The longitudinal confinement (along the cavity axis) introduces a large frequency spacing between adjacent longitudinal modes and modifies spontaneous emission coupling such that basically only photons of longitudinal mode number $q = 7$ (Fig. 1a) are observed to populate the cavity. By this, an effective low frequency cutoff ω_{cutoff} (the eigenfrequency for the corresponding TEM_{00} transverse mode) is introduced, with $\hbar\omega_{\mathrm{cutoff}} \sim 2.1\,\mathrm{eV}$, much larger than the thermal energy $k_{\mathrm{B}}T$ ($\sim 1/40\,\mathrm{eV}$ at room temperature). The two remaining transverse modal degrees of freedom of light thermalize to the (internal rovibrational) temperature of the dye solution, and the photon frequencies will be distributed by an amount $\sim k_{\mathrm{B}}T/\hbar$ above the cavity cutoff. We expect significant population for the TEM_{nm} modes with high transversal quantum numbers n and m (of high eigenfrequency) at high temperature, whereas the population concentrates to the lower transverse modes when the system is cold. Equilibrium is reached as photons are absorbed and emitted by dye molecules many times, with the interplay between fluorescence and absorption leading to a thermal population of cavity modes, making the photon gas equilibrate at the temperature of the dye solution (see the Methods section). During the course of thermalization (in an idealized experiment) only transverse mode quantum numbers are varied, and—different from in experiments observing blackbody radiation[9,18]—no photons are destroyed or created on average. This becomes clear by noting that the dye molecules have quantized electronic excitation levels with a transition energy near or above the cutoff, and thermal excitation is suppressed by a factor of order $\exp(-\hbar\omega_{\mathrm{cutoff}}/k_{\mathrm{B}}T) \sim 10^{-36}$.

The thermodynamics of the system can readily be obtained by a mapping onto the two-dimensional ideal Bose gas: for paraxial propagation and a fixed longitudinal excitation number, photons can be treated as non-relativistic massive particles with mass $m_{\mathrm{ph}} = \hbar\omega_{\mathrm{cutoff}}/c^2$ (see the Methods section), moving in the transverse plane of the resonator[12]. Owing to the curvature of the mirrors, the photons are moreover under harmonic confinement (see the Methods section). When the photons are in thermal equilibrium and their average number is conserved, we expect that this trapped two-dimensional ideal Bose gas will undergo a phase transition to a Bose–Einstein condensate at sufficiently low temperature and high density[19,20]. A notable further consequence of the thermalization of the trapped photon gas is an accumulation in the trap centre, where the photon trapping potential is minimum. This behaviour is evident from the analogy to a trapped gas of material particles.

Our experimental set-up shown in Fig. 1b is based on an optical resonator consisting of two high-reflecting curved optical mirrors spaced 3.5 optical wavelengths apart, filled with dye solution (see the Methods section). The short distance between the cavity mirrors yields a free spectral range ($\sim 7 \times 10^{13}\,\mathrm{Hz}$) much larger than the thermal energy $k_{\mathrm{B}}T$ in frequency units ($\sim 6 \times 10^{12}\,\mathrm{Hz}$ at room temperature), and comparable to the spectral width of the dye emission. The mean transversal excitation number (per axis) of the two-dimensional photon gas is $k_{\mathrm{B}}T/\hbar\Omega \sim 160$, where $\Omega/2\pi$ ($\sim 4 \times 10^{10}\,\mathrm{Hz}$) denotes the spacing of transversal cavity modes; that is, the spacing is so small that the transverse motion is quasicontinuous. Other than in a perfect 'photon box'[21] we expect losses from coupling to optical modes not confined in the cavity, non-radiative decay and mirror losses. To compensate for the loss rate, the dye is pumped with an external laser beam. In a simple model, the pumping fills a reservoir of electronic excitations in the dye that can exchange particles with the photon gas. Thus, the photon gas is seen as an open system, in the sense of a grand-canonical ensemble. The pumping maintains a steady

Institut für Angewandte Physik, Universität Bonn, Wegelerstr. 8, 53115 Bonn, Germany. *e-mail: Martin.Weitz@uni-bonn.de.

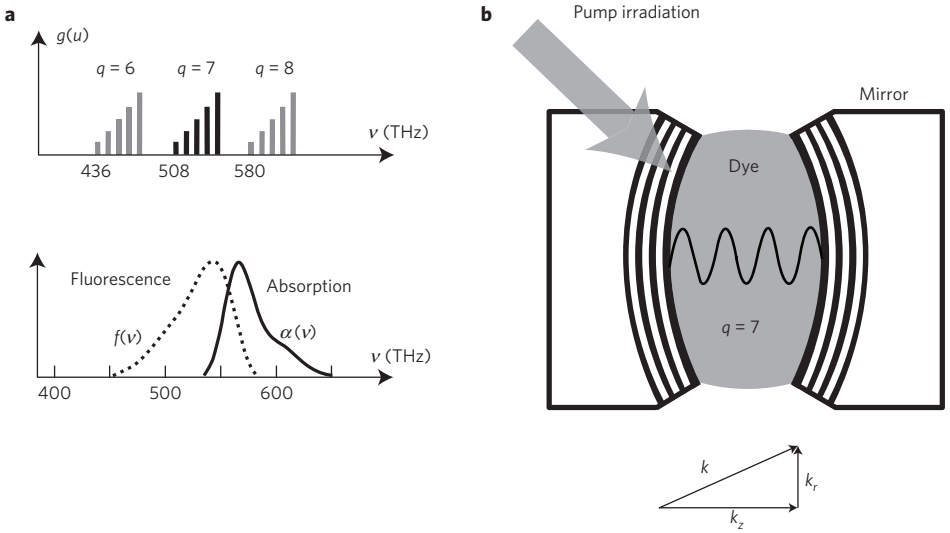

Figure 1 | Cavity mode spectrum and set-up. a, Schematic spectrum of cavity modes. Transverse modes belonging to the manifold of longitudinal mode number $q = 7$ are shown by black lines, those of other longitudinal mode numbers in grey. (508 THz is equivalent to a wavelength of 590 nm.) The energy of an eigenmode in the $q = 7$ manifold is $\varepsilon = \hbar\omega_{\mathrm{cutoff}} + u$ with transversal energy $u = \hbar\Omega(n_x + n_y)$, transversal excitation numbers n_x, n_y and frequency splitting Ω between transversal modes[29]. The degeneracy $g(u) = 2(u/\hbar\Omega + 1)$ of a given transversal energy exhibits a linear energy scaling, and the prefactor two originates from the two possible polarizations. The bottom graph indicates the (measured) relative absorption coefficient and fluorescence strength of rhodamine 6G dye versus frequency. **b**, Experimental set-up for thermalization of a two-dimensional photon gas.

state in which the average photon number N_{ph} will be proportional to the number of electronic excitations N_{exc} and is determined by $N_{\mathrm{ph}}/N_{\mathrm{exc}} = \tau_{\mathrm{ph}}/\tau_{\mathrm{exc}}$, where τ_{ph} and τ_{exc} denote the lifetimes of photons and electronic excitations, respectively. Despite losses and pumping we expect the photon gas to be well described by an equilibrium distribution when the thermalization is sufficiently fast; that is, a photon scatters several times off a molecule before being lost. Our present experiment is carried out at an optical pumping beam intensity of $\sim$10 W cm^{-2}, an estimated three orders of magnitude below the onset of a photon Bose–Einstein condensate and four orders of magnitude below saturation, so that we do not expect collective photonic effects to be relevant.

Experimental data for the spectral distribution of light transmitted by one of the cavity mirrors are shown in Fig. 2a for two different temperatures of the resonator. The connected circles represent experimental data, and the solid lines are theoretical curves for a fully thermalized gas at the corresponding temperature. The expected photon number in the cavity $n_{T,\mu}(u)$ at given transversal energy $u = \varepsilon - \hbar\omega_{\mathrm{cutoff}}$ is the product of the energy degeneracy $g(u) = 2(u/\hbar\Omega + 1)$ (Fig. 1a) and the Bose–Einstein distribution factor:

$$n_{T,\mu}(u) = \frac{g(u)}{\exp\left(\frac{u-\mu}{k_{\mathrm{B}}T}\right) - 1} \qquad (1)$$

The chemical potential μ is determined by measuring the output power $P_{\mathrm{out}} = 50 \pm 5$ nW, which corresponds to a photon number of $N_{\mathrm{ph}} = 60 \pm 10$ in the cavity, and solving $\sum_u n_{T,\mu}(u) = N_{\mathrm{ph}}$ for μ. For the two cases in Fig. 2a we obtain $\mu/k_{\mathrm{B}}T = -6.76 \pm 0.17$ ($T = 300$ K) and $\mu/k_{\mathrm{B}}T = -7.16 \pm 0.17$ ($T = 365$ K) respectively. As a result of $\mu \ll -k_{\mathrm{B}}T$, the term -1 in the denominator of equation (1) can be neglected and the distribution becomes Boltzmann-like, with the term $e^{\mu/k_{\mathrm{B}}T}$ acting as a prefactor to the spectral distribution. A Bose–Einstein condensate would be expected for $N_{\mathrm{ph}} \to N_{\mathrm{c}} = \sum_{u>0} n_{T,\mu=0}(u) = (\pi^2/3)(k_{\mathrm{B}}T/\hbar\Omega)^2 \approx$ 80,400 (at which $\mu \to 0$). The shapes of the shown experimental spectra are in good agreement with theoretical expectations over a wide spectral range (a visible deviation near 532 nm stems from residual pump light). Notably, the enhancement of the short-wavelength wing for the higher temperature data by almost an order of magnitude is predicted accurately. We interpret these results as one line of evidence for the two-dimensional photon gas to be in thermal equilibrium with the dye solution. Evidence is also obtained from investigating the spatial distribution of light emitted by the resonator. A typical snapshot is shown in Fig. 2b, in which a shift from the yellow spectral regime for light near the axis towards the green (that is, higher photon energy) for the radiation emitted off-axis is clearly visible. This is due to the higher energy of cavity resonances with a large transversal momentum and correspondingly large mode diameter. From the image in Fig. 2b, the spatial intensity distribution shown in Fig. 2c was extracted, which is in good agreement with a thermal average over spatial modes. In other words, the thermal distribution of the photon spectrum is also reflected by the spatial distribution.

In further measurements, we have varied the cutoff wavelength $\lambda_{\mathrm{cutoff}} = 2\pi c/\omega_{\mathrm{cutoff}}$ by piezo tuning of the distance between cavity mirrors. A series of corresponding spectra is shown in Fig. 3a. Reasonable agreement with a thermal distribution is obtained for the two spectra shown at the top with cutoff wavelengths near 570 and 590 nm respectively, whereas the two spectra with longer cutoff wavelengths shown in the bottom seem only partly thermalized. We attribute this to weak dye reabsorption in this spectral regime, preventing repeated photon scattering off the dye molecules (also the reflectivity of cavity mirrors lessens at wavelengths above 600 nm). This illustrates the importance of both emission and reabsorption of scattered photons for thermalization, in agreement with expectations.

Finally, thermalization was investigated by varying the spatial position of the external pumping beam with respect to the centre of the trapping region. Figure 3b shows the position of the maximum of the emitted fluorescence x_{max} versus the transverse position of the pump focus x_{exc} for two different values of the cutoff wavelength. For the data recorded with a cutoff wavelength near 580 nm (squares fitted with a solid line) the fluorescence essentially freezes to the position of the trapping centre, when the excitation spot is closer than approximately 60 µm distance. This effect is not observed when tuning the cutoff wavelength to 620 nm (circles fitted with a dashed line), where weak reabsorption prevents

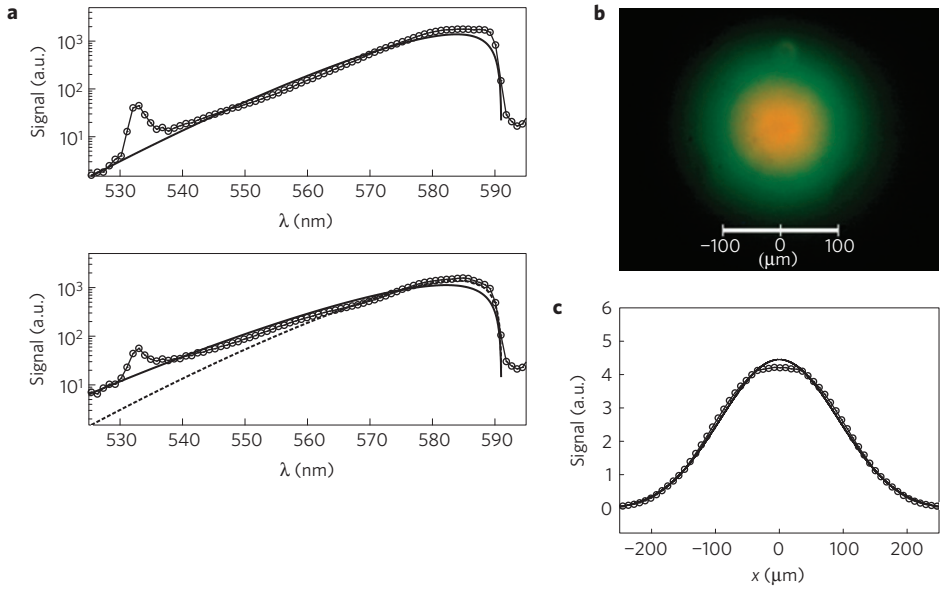

Figure 2 | Experimental spectra and intensity distribution. a, The connected dots give measured spectral intensity distributions for temperatures of 300 K (top) and 365 K (bottom) of the resonator set-up. The solid lines are theoretical spectra based on Bose–Einstein-distributed transversal excitations, and for illustration a $T = 300$ K distribution is also inserted in the bottom graph (dashed line). The measurements shown in this figure were carried out with rhodamine 6G dye dissolved in ethylene glycol ($c = 5 \times 10^{-4}$ M). Note that the spectral maximum of blackbody radiation at $T = 300$ K is at ~10 μm wavelength, that is, far to the red of the shown spectral regime. **b**, Image of the radiation emitted along the cavity axis at room temperature ($T = 300$ K), showing a shift towards shorter (higher energetic) optical wavelengths for off-axis radiation. **c**, Spatial intensity distribution at $T = 300$ K (connected circles) along with the theoretical prediction (solid line).

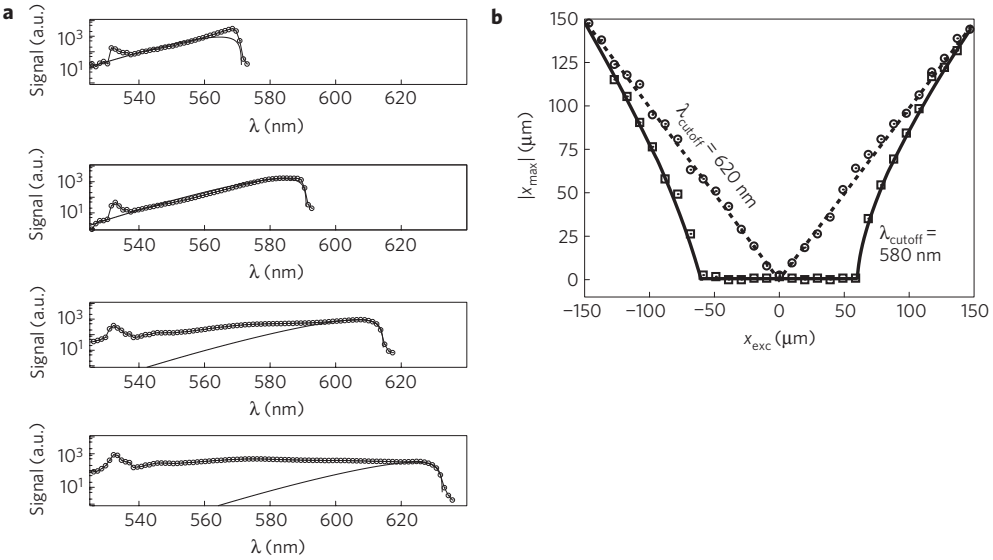

Figure 3 | Break-down of thermalization. a, Measured spectral intensity distribution for different cavity cutoff wavelengths (connected dots) overlaid with theory curves (solid lines). For the two spectra with longer cutoff wavelengths, the visible deviation from a thermal spectrum is attributed to weak dye reabsorption in this spectral regime (rhodamine 6G in ethylene glycol, $c = 5 \times 10^{-4}$ M). **b**, Measured distance of the intensity maximum of the emitted radiation $|x_{max}|$ from the centre versus position of the excitation spot x_{exc}. For the data recorded with $\lambda_{cutoff} \approx 580$ nm (squares fitted with a solid line) a position locking to the cavity centre is observed, whereas the fluorescence follows the excitation spot when tuning to weak reabsorption ($\lambda_{cutoff} \approx 620$ nm, circles fitted with a dashed line) (perylene diimide dissolved in acetone, $c = 0.75\ \mathrm{g\,l^{-1}}$).

multiple scattering events and thus an efficient thermalization (Fig. 3a). The demonstrated position locking effect is a direct consequence of the thermalization, leading to a photon accumulation at the trap centre, where the confining potential imposed by the curved mirrors exhibits a minimum value. We attribute the observed breakdown of thermalization for data points with $|x_{exc}| > 60\,\mu$m to the finite quantum efficiency of the dye ($\eta \cong 95\%$; ref. 22), and our mirrors providing only a one-dimensional photonic bandgap, limiting the number of possible photon scattering processes. The relaxation also for initial states further apart from equilibrium could be improved with mirrors providing a full three-dimensional photonic bandgap[23]. Technical applications of the observed directed diffusion effect could include the collection of diffuse solar light to a central spot[14], with prospects for enhancing the optical phase space density. When a Bose–Einstein condensate of photons can be reached, perspectives include coherent ultraviolet sources[24].

Methods

Experimental set-up. Our optical resonator consists of two high-reflecting dielectric mirrors with spherical curvature ($R = 1$ m). One of the mirrors is cut to 1 mm × 1 mm surface size to allow for a distance between mirrors in the micrometre regime ($D_0 \cong 1.46\,\mu$m) despite the mirrors' curvature. The measured reflectivity of the cavity mirrors is ~99.9985% in the relevant wavelength regime (520–590 nm). The resonator is filled with a drop of dye (rhodamine 6G or perylene diimide respectively) dissolved in an organic solvent and is pumped with a laser beam near 532 nm wavelength inclined at 45° to the cavity axis, exploiting a reflectivity minimum.

Photon dispersion in cavity. The photon energy as a function of transversal (k_r) and longitudinal (k_z) wavenumber in the paraxial approximation ($k_z \gg k_r$) is $E = \hbar c\sqrt{k_z^2 + k_r^2} \cong \hbar c(k_z + k_r^2/2k_z)$, with c as the speed of light in the medium. Within the resonator, we have $k_z(r) = q\pi/D(r)$ with $D(r) = D_0 - 2(R - \sqrt{R^2 - r^2})$ as the mirror separation at distance r from the axis. For $r \ll R$ and a fixed longitudinal mode number q one finds

$$E \cong m_{\mathrm{ph}}c^2 + \frac{(\hbar k_r)^2}{2m_{\mathrm{ph}}} + \frac{1}{2}m_{\mathrm{ph}}\Omega^2 r^2$$

We arrive at the dispersion of a particle with mass $m_{\mathrm{ph}} = \hbar k_z(0)/c = \hbar\omega_{\mathrm{cutoff}}/c^2$ subject to a harmonic oscillator potential of trapping frequency $\Omega = c/\sqrt{D_0 R/2}$ in two spatial dimensions.

Principle of radiation field thermalization. For photons absorbed and emitted by dye molecules many times, the state of the light field can be regarded as following a random walk in configuration space. For a transition between two configurations, P and Q (that is, sets of mode occupation numbers), induced by the absorption of a photon in mode i and the emission into mode j, the transition rate is expected to follow $R(P \to Q) \propto \alpha_T(\omega_i) f_T(\omega_j)$ with $\alpha_T(\omega)$ and $f_T(\omega)$ as (temperature dependent) relative absorption and fluorescence strength coefficients. This random walk in configuration space will lead to a thermal equilibrium population of photon modes, if the condition of detailed balance[25] is fulfilled:

$$\frac{R(P \to Q)}{R(Q \to P)} = \frac{\alpha_T(\omega_i) f_T(\omega_j)}{\alpha_T(\omega_j) f_T(\omega_i)} = \exp\left(-\frac{\hbar(\omega_j - \omega_i)}{k_{\mathrm{B}}T}\right) \qquad (2)$$

Dye spectra are known to typically fulfil (2) within good accuracy, which itself is a consequence of a thermal equilibrium of rovibrational excitations within the ground and excited electronic molecular levels respectively[26–28].

For a simple model of the thermalization process in the dye, consider a two-level system with energy splitting $\hbar\omega_0$ subject to further rovibrational sublevel structures of ground and excited state[28]. Absorption $\alpha_T(\omega)$ and fluorescence strength $f_T(\omega)$ at frequency ω can be expanded by integrating over the contributions from individual energetic sublevels, yielding a ratio

$$\frac{f_T(\omega)}{\alpha_T(\omega)} \propto \frac{\int g'(e')p(e')A(e',\omega)\,\mathrm{d}e'}{\int g(e)\exp(-e/k_{\mathrm{B}}T)B(e,\omega)\,\mathrm{d}e}$$

where e and e' denote the energies of sublevels of ground and excited electronic state respectively, $p(e')$ the population of sublevels in the excited electronic state, g and g' the density of states and A and B are the Einstein coefficients. The Einstein coefficients at sublevels with energies e and e' matching $\hbar\omega + e = \hbar\omega_0 + e'$ are connected by the A–B relation $g'(e')A(e',\omega)\,\mathrm{d}e' = (2\hbar\omega^3/\pi c^2)g(e)B(e,\omega)\,\mathrm{d}e$. When thermalization in the electronically excited molecular level is sufficiently fast, $p(e') \propto \mathrm{e}^{-e'/k_{\mathrm{B}}T} = \mathrm{e}^{-(e+\hbar(\omega-\omega_0))/k_{\mathrm{B}}T}$ and one immediately finds $f_T(\omega)/\alpha_T(\omega) \propto \omega^3 \mathrm{e}^{-\hbar(\omega-\omega_0)/k_{\mathrm{B}}T}$. With this, the detailed balance condition (2) relating absorption and fluorescence at two different frequencies is fulfilled for $\hbar\omega \gg k_{\mathrm{B}}T$.

Received 23 December 2009; accepted 21 April 2010; published online 30 May 2010

References

1. Einstein, A. Quantentheorie des einatomigen idealen Gases. *Zweite Abhandlung. Sitz.ber. Preuss. Akad. Wiss.* **1,** 3–14 (1925).
2. Anderson, M. H., Ensher, J. R., Matthews, M. R., Wieman, C. E. & Cornell, E. A. Observation of Bose–Einstein condensation in a dilute atomic vapor. *Science* **269,** 198–201 (1995).
3. Davis, K. B., Mewes, M-O., Andrews, M. R., van Druten, N. J., Kurn, D. M. & Ketterle, W. Bose–Einstein condensation in a gas of sodium atoms. *Phys. Rev. Lett.* **75,** 3969–3973 (1995).
4. Bradley, C. C., Sackett, C. A. & Hulet, R. G. Bose–Einstein condensation of lithium: Observation of limited condensate number. *Phys. Rev. Lett.* **78,** 985–989 (1997).
5. Jochim, S. *et al.* Bose–Einstein condensation of molecules. *Science* **302,** 2101–2103 (2003).
6. Deng, H., Weihs, G., Santori, C., Bloch, J. & Yamamoto, Y. Condensation of semiconductor microcavity exciton polaritons. *Science* **298,** 199–2002 (2002).
7. Kasprzak, J. *et al.* Bose–Einstein condensation of exciton polaritons. *Nature* **443,** 409–414 (2006).
8. Balili, R., Hartwell, V., Snoke, D., Pfeiffer, L. & West, K. Bose–Einstein condensation of microcavity polaritons in a trap. *Science* **316,** 1007–1010 (2007).
9. Planck, M. Über das Gesetz der Energieverteilung im Normalspectrum. *Ann. Phys.* **4,** 553–563 (1901).
10. Huang, K. *Statistical Mechanics* 2nd edn, 293–294 (Wiley, 1987).
11. Van Sark, W. G. J. H. M. *et al.* Luminescent solar concentrators—a review of recent results. *Opt. Exp.* **16,** 21773–21792 (2008).
12. Chiao, R. Y. Bogoliubov dispersion relation for a 'photon fluid': Is this a superfluid? *Opt. Commun.* **179,** 157–166 (2000).
13. Bolda, E. L., Chiao, R. Y. & Zurek, W. H. Dissipative optical flow in a nonlinear Fabry–Pérot cavity. *Phys. Rev. Lett.* **86,** 416–419 (2001).
14. Mitchell, M. W., Hancox, C. I. & Chiao, R. Y. Dynamics of atom-mediated photon–photon scattering. *Phys. Rev. A* **62,** 043819 (2000).
15. Jhe, W. *et al.* Suppression of spontaneous decay at optical frequencies: Test of vacuum-field anisotropy in confined space. *Phys. Rev. Lett.* **58,** 666–669 (1987).
16. De Martini, F., Jacobovitz, G. R. & Mataloni, P. Anomalous spontaneous emission time in a microscopic optical cavity. *Phys. Rev. Lett.* **59,** 2955–2958 (1987).
17. De Martini, F. & Jacobovitz, G. R. Anomalous spontaneous–stimulated-decay phase transition and zero-threshold laser action in a microscopic cavity. *Phys. Rev. Lett.* **60,** 1711–1714 (1988).
18. Raimond, J. M., Goy, P., Gross, M., Fabre, C. & Haroche, S. Collective absorption of blackbody radiation by Rydberg atoms in a cavity: An experiment on Bose statistics and Brownian motion. *Phys. Rev. Lett.* **49,** 117–120 (1982).
19. Bagnato, V. & Kleppner, D. Bose–Einstein condensation in low-dimensional traps. *Phys. Rev. A* **44,** 7439–7441 (1991).
20. Mullin, W. J. Bose–Einstein condensation in a harmonic potential. *J. Low Temp. Phys.* **106,** 615–641 (1997).
21. Bohr, N. in *Albert Einstein: Philosopher–Scientist* (ed. Schilpp, P. A.) (The Library of Living Philosophers, Vol. VII, Open Court. La Salle, 1949).
22. Magde, D., Wong, R. & Seybold, P. G. Fluorescence quantum yields and their relation to lifetimes of rhodamine 6G and fluorescein in nine solvents: Improved absolute standards for quantum yields. *Photochem. Photobiol.* **75,** 327–334 (2002).
23. Noda, S., Tomoda, K., Yamamoto, N. & Chutinan, A. Full three-dimensional photonic bandgap crystals at near-infrared wavelengths. *Science* **289,** 604–606 (2000).
24. Jonkers, J. High power extreme ultra-violet (EUV) light sources for future lithography. *Plasma Sources Sci. Technol.* **15,** S8–S16 (2006).
25. Metropolis, N., Rosenbluth, A. W., Rosenbluth, M. N., Teller, A. H. & Teller, E. Equation of state calculations by fast computing machines. *J. Chem. Phys.* **21,** 1087–1092 (1953).
26. Kennard, E. H. The excitation of fluorescence in fluorescein. *Phys. Rev.* **29,** 466–477 (1927).
27. McCumber, D. E. Einstein relations connecting broadband emission and absorption spectra. *Phys. Rev.* **136,** A954–A957 (1964).
28. Sawicki, D. A. & Knox, R. S. Universal relationship between optical emission and absorption of complex systems: An alternative approach. *Phys. Rev. A* **54,** 4837–4841 (1996).
29. Kogelnik, H. & Li, T. Laser beams and resonators. *Appl. Opt.* **5,** 1550–1567 (1966).

Acknowledgements

We thank F. Schelle for experimental contributions during the early phase of this project. Financial support from the Deutsche Forschungsgemeinschaft within the focused research unit FOR557 is acknowledged.

Author contributions

J.K. and M.W. contributed to the experimental idea; J.K. carried out the experiments. All authors analysed the experimental data and discussed the results.

Additional information

The authors declare no competing financial interests. Reprints and permissions information is available online at http://npg.nature.com/reprintsandpermissions. Correspondence and requests for materials should be addressed to M.W.